Title

Scale-Up of Novel Li-Conducting Halide Solid State Battery Electrolyte

Author

Tucker, Michael

Publication Date

2025-03-18

Cooperative Research and Development Agreement (CRADA) Final Report

Report Date: 3/18/2025

In accordance with Requirements set forth in the terms of the CRADA, this document is the CRADA Final Report, including a list of Subject Inventions. It is to be forwarded to the DOE Office of Scientific and Technical Information upon completion or termination of the CRADA, as part of the commitment to the public to demonstrate results of federally funded research.

Parties to the Agreement: Lawrence Berkeley National Laboratory and Saint-Gobain Northboro Research and Development Center

CRADA number: FP00011705

CRADA Title: Scale-Up of Novel Li-Conducting Halide Solid State Battery Electrolyte

Responsible Technical Contact at Berkeley Lab: Michael Tucker

Name and Email Address of POC at Partner Company(ies):
John Pietras, John.D.Pietras@saint-gobain.com

Sponsoring DOE Program Office(s):
DOE-EERE-VTO

LBNL Report Number:
LBNL-2001659

OSTI Number:
[SPO to complete]

Joint Work Statement Funding Table showing DOE funding commitment:

DOE Funding to LBNL	1,200,000.00
Participant Funding to LBNL	0
Participant In-Kind Contribution Value	1,200,000.00
Total of all Contributions	2,400,000.00

Provide a list of publications, conference papers, or other public releases of results, developed under this CRADA:

F. Shen, M. McGahan, J.D. Pietras, G.Y. Lau, M.M. Doeff, V.S. Battaglia, M.C. Tucker, 2025, Optimization of catholyte for halide-based all-solid-state batteries, J. Power Sources, 640 (236709) https://doi.org/10.1016/j.jpowsour.2025.236709

F. Shen, M. McGahan, J.D. Pietras, G.Y. Lau, M.M. Doeff, V.S. Battaglia, M.C. Tucker, 2023, Tape casting of thin electrolyte and thick cathode for halide-based all-solid-state batteries, J. Electrochemical Society, 170 (100505) doi.org/10.1149/1945-7111/acfdd1

F. Shen, M. McGahan, J.D. Pietras, G.Y. Lau, M.M. Doeff, V.S. Battaglia, M.C. Tucker, 2024, Halide-Based All-Solid-State Batteries: From Pellet Cells to Pouch Cells, PRiME 2024, 10/8/2024

M.C. Tucker, F. Shen, V. Battaglia, M.M. Doeff, 2023, Scale up of Halide Solid State Batteries, VTO Annual Merit Review, 6/4/2024

F. Shen, M. McGahan, J.D. Pietras, G.Y. Lau, M.M. Doeff, V.S. Battaglia, M.C. Tucker, 2024, Scale-Up of Halide-Based All-Solid-State Batteries, 2024 MRS Spring Meeting, 4/24/2024

F. Shen, M. McGahan, J.D. Pietras, G.Y. Lau, M.M. Doeff, V.S. Battaglia, M.C. Tucker, 2024, Halide-Based All-Solid-State Batteries, Solid-State Battery Summit, 8/14/2024

F. Shen, M. McGahan, J.D. Pietras, G.Y. Lau, M.M. Doeff, V.S. Battaglia, M.C. Tucker, 2023, Tape cast thin electrolyte and thick cathode for halide-based all-solid-state batteries, 2023 MRS Spring Meeting, 4/11/2023

Provide a detailed list of all subject inventions, to include patent applications, copyrights, and trademarks:

NONE

Executive Summary of CRADA Work:

LBNL and project partner Saint Gobain (SG) demonstrated scalable processing of halide-based solid state batteries. SG’s innovative halide-based SSE utilized in this project is inherently scalable: it can be compressed into a dense electrolyte sheet at room temperature under moderate pressure, can be processed in dry air, and does not present any safety issues during processing or end use. The halide material forms the dense electrolyte layer, and is dispersed in the thick cathode to form a highly conductive path for Li ions. The halide also comes in contact with various environments and other materials (solvents, binders, processing equipment, etc.) throughout the battery manufacturing process, and must be stable in contact with cathode and anode materials during operation. R&D efforts commonly use thick pellets of SSE materials to interrogate the relevant interactions, however such studies do not usually reflect the challenges and processing constraints of commercially-relevant thin electrolyte layers. To establish the scalability of this promising material, full cells were fabricated using a thin electrolyte layer and scalable processing techniques. Issues encountered during scale-up and processing were thoroughly characterized and addressed, providing a basis for pilot manufacturing to commence.

This project benefits the public by increasing confidence in and providing guidance for utilization of a promising new class of solid state battery material. This material is expected to impact the transportation and portable battery markets. This project surpassed the state of the art, by demonstrating for the first time full cells comprising electrolyte and cathode layers with practical thicknesses, utilizing the industrial scalable tape casting process. Suitable commercially-available binders and solvents were identified, suggesting feasibility of further scale-up.

Summary of Research Results:

Various aspects of halide cell processing and materials were developed. Compatibility studies indicated that the halide material is compatible with toluene, but not with most other common tape-casting solvents. Binder MSB1-13 was down-selected from more than 10 candidates for halide tape casting. A loading of 2 to 3wt% MSB1-13 binder was used for tape casting halide electrolyte according to a trade-off between ionic conductivity and mechanical properties. A CAM was selected and the cathode components ratio was optimized. The catholyte particle size and loading plays an important role, with a clear tradeoff between high rate capability (at lower CAM loading) and high energy density (at higher CAM loading). Sub-micron catholyte particles provide greatly improved C-rate capability, even at high loading. Optimized cathode mixtures and electrolyte layers were successfully tape cast, and demonstrated in a scaled-up 3x4 cm cell which cycled 30 times without short circuiting. Various anode interlayer materials were evaluated, and a full cell with LPSCl between the Li metal and halide electrolyte was successfully cycled. Future work should focus on further optimizing the cathode tape, increasing the capacity of pouch cells, and evaluation of alternative anode interlayer materials.

Binder selection and loading

Binders used in the battery industry, such as polyvinylidene fluoride (PVDF), and many common tape casting binders, such as polyvinyl acetate (PVA) or polyvinyl butyral (PVB), do not dissolve in toluene. More than 10 candidate binders were ball milled separately with LYB powder in toluene. All the selected binders, QPAC100, QPAC130, ethyl cellulose, PEO, PMMA, polyethylenimine, MSB1-13, polystyrene, polybutadiene and poly(acrylonitrile-co-butadiene) show good compatibility with LYB. The ionic conductivity of the LYB tapes is 1 to 4 orders of magnitude lower than the fresh powder, depending on the binder type and content. The tapes with PEO, polyethylenimine, MSB1-13, polystyrene or poly(acrylonitrile-co-butadiene) as the binder show good ionic conductivity (Table 1). Considering mechanical properties, such as strength, elongation, flexibility and robustness after lamination, MSB1-13 was selected as the binder for further tape casting optimization.

Table 1. Ionic conductivity of LYB tapes with binders, cast from toluene slurries.

Binder	**Ionic conductivity (S cm^{-1})**	**Tape quality**
2% QPAC100+1.7% polycarbonate	3.4×10^{-5}	Cracked
3% QPAC130	9.7×10^{-5}	Brittle
2.5% ethyl cellulose (300 cP)	9.1×10^{-5}	Cracked
3% PEO	1.5×10^{-4}	Brittle
3% PMMA	1.0×10^{-5}	Brittle
2.5% polyethylenimine	2.2×10^{-4}	Cracked
2% MSB1-13	2.0×10^{-4}	Flexible
2.5% polystyrene	3.2×10^{-4}	Brittle
3% polystyrene	1.4×10^{-4}	Brittle
3% polybutadiene	6.2×10^{-6}	Flexible
3% poly(acrylonitrile-co-butadiene)	1.1×10^{-4}	Flexible

The impact of MSB1-13 content on tape quality and ionic conductivity is shown in Figure 1. With increasing binder content there is a trade-off: mechanical properties improve significantly, but ionic conductivity decreases approximately logarithmically. At 1 and 1.5 wt% MSB1-13 loading, the tapes are very challenging to peel off from the Al substrate. When the binder content is increased to 2 wt%, the tape is still not free-standing in large area but it can be peeled off from the Al substrate when it is punched into a small area (<1.6 cm^2). Large area tapes could be successfully stripped from the substrate by first laminating with a cathode tape. When the binder content is further increased to 5 wt% or 10 wt%, large-area free-standing tapes are achieved, but with an unacceptable sacrifice of ionic conductivity.

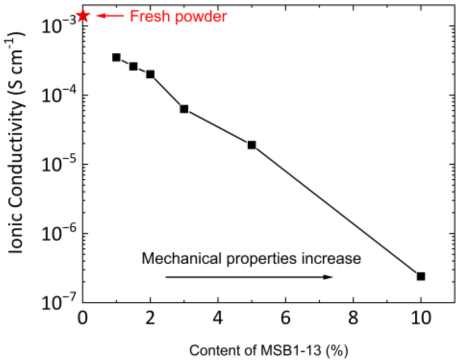

Figure 1. Impact of binder loading for MSB1-13. Ionic conductivity vs. MSB1-13 content.

Several NMC cathode active material (CAM) candidates were compared and single crystal NMC811 with a particle size of 3 to 5 µm from MSE Supplies LLC was selected. The ratio of the cathode components was also optimized. Results show that 70% NMC811 with 29% raw Gen2.2

catholyte and 1% C65 is optimal. Saint-Gobain also provided Gen2.2 powder with particle size decreased from ~20 µm to ~3 µm. Replacing the raw Gen2.2 catholyte with fine Gen2.2 catholyte, the capacity increased. With 24 wt% catholyte, the capacity increased from 120 mAh/g for raw Gen2.2 catholyte to 169 mAh/g for fine Gen2.2 catholyte. Even with 19 wt% fine Gen2.2 catholyte, the capacity is 145 mAh/g at 0.05 C. Less catholyte is needed when the catholyte particle size is smaller, thereby improving energy density. To further decrease particle size, we synthesized Li_3InCl_6 (LIC) with particle size less than 500 nm, even smaller than the fine Gen2.2 particle size. Cells were prepared with very fine halide as catholyte (LIC) and fine halide as separator (Gen2.2). With fine Gen2.2 catholyte replaced by LIC and a cathode interlayer loaded between cathode and pellet electrolyte, the cell shows discharge capacity of 186, 169, 153 and 122 mAh/g at 0.02, 0.05, 0.1 and 0.2 C, respectively. The cathode was composed of 80% NMC811, 19% LIC and 1% C65. After cycling at different C rates, the cell was further cycled at a constant C rate of 0.1 C for almost 40 cycles. The retention is 55% and the coulombic efficiency is ~97% (Figure 2). LIC catholyte provides better ionic conduction in the cathode due to the smaller particle size.

Cathode optimization

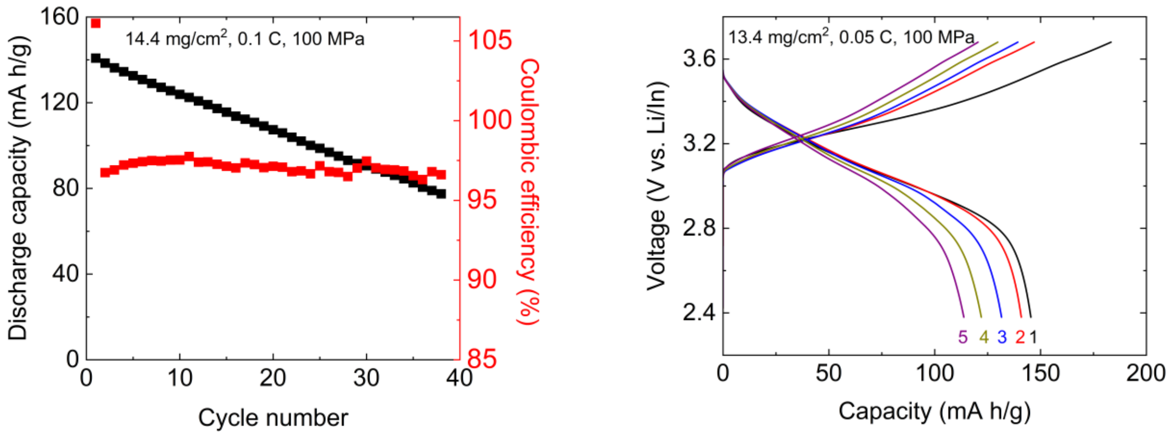

Figure 2. (Left) The retention of a pellet cell with LIC catholyte and cathode interlayer in ~40 cycles at 0.1 C. Cell structure: Li-In(150µm)/Gen2.2(300µm)/LIC(300µm)/NMC-LIC-C(100µm). (Right) Charge/discharge curves of a tape cast cell with cell structure: Li-In(150µm)/Gen2.2-MSB(40µm)/LIC-MSB(40µm)/NMC-LIC-C-MSB(100µm).

A systematic study with different catholytes was conducted, focusing on the catholyte particle size, Fig. 3. Raw Gen2.2 LYBC (20 µm), milled Gen2.2 LYBC (3 µm) and nano Li3InCl6 LIC (0.4 µm) catholytes were added to the NMC (LiNi0.83Mn0.06Co0.11O2) cathode active material (CAM). It is challenging to further mill Gen2.2 catholyte to the sub-micron scale, so fine LIC with a similar ionic conductivity as the milled Gen2.2 was adopted. The ratio of CAM and catholyte was varied (85/14, 80/19, 75/24, 70/29 wt%), with the content of carbon C65 fixed to 1 wt%. At moderate CAM loading (70 wt%) and 0.1 C-rate, all the three catholytes perform well, providing initial discharge capacities >177 mAh/g with the highest capacity improved to 193 mAh/g at 0.1 C and 20 °C. At high CAM loading (85 wt%) and 0.1 C-rate, a cathode with LIC catholyte provides discharge capacity of 175 mAh/g, while the larger particle size catholytes suffer significantly reduced capacity. Reducing the particle size of the halide catholyte enhances the discharge capacity of the cells at high CAM loading (85 wt%) or high C-rate cycling. These results imply that cathode particle size is critically important for performance at high CAM loading.

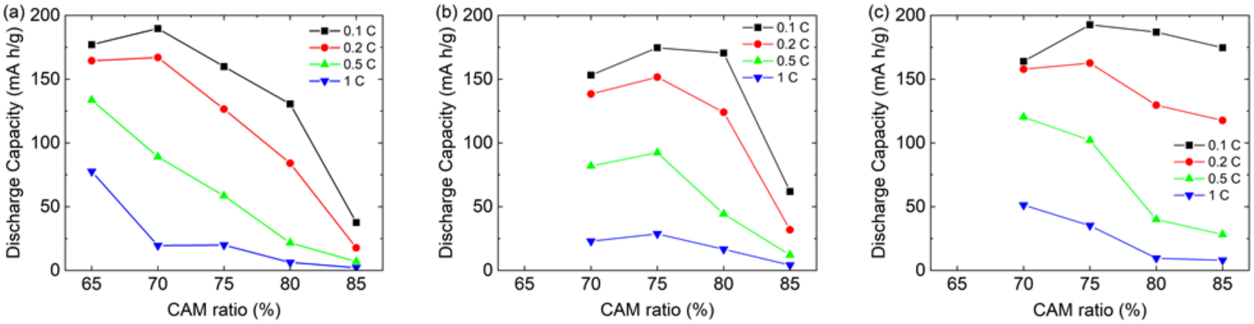

Figure 3. Discharge capacities of cells with different CAM ratio and (a) raw Gen2.2, (b) milled Gen2.2 and (c) sub-micron LIC catholytes. Cells were composed of cathode (CAM loading: 14 mg/cm2), milled Gen2.2 electrolyte (80 mg, ~600 µm) and Li/In alloy anode (80 µm). Cells were cycled at 100 MPa and 20 °C.

Selected cells were cycled between 3-4.4V vs. Li/Li^+, and one representative is shown in Fig. 4. The cell maintains 75% of the first-cycle capacity after 200 cycles, and Coulombic efficiency above 99.5%.

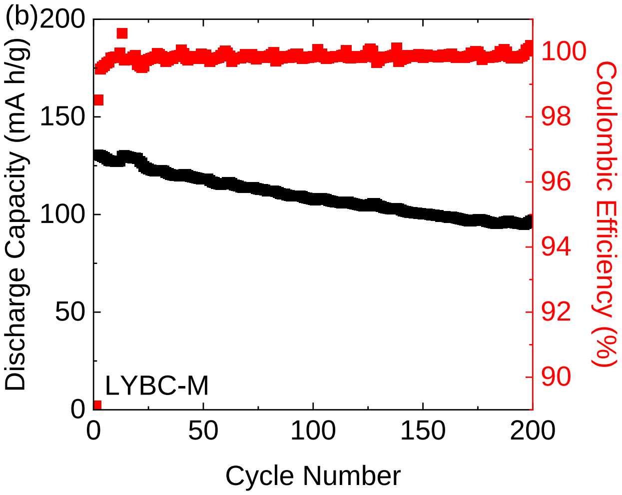

Figure 4. Li-In(80µm)/Gen2.2 pellet (600µm)/NMC-milled Gen2.2-C(80µm) cell structure. Retention of a cell with 29% of the milled Gen2.2 cathode at 0.2 C and room temperature.

Anode interlayer

The halide electrolyte is compatible with NMC cathode and LiIn anode, but Li metal anode is preferred to increase energy density. Unfortunately, the halide is not electrochemically stable in contact with Li metal, so anode interlayer materials were explored. Several candidates were evaluated for conductivity, and stability in Li/interlayer/halide/interlayer/Li symmetric cells. Based on these results, Li3N and argyrodite LPSCl were selected for demonstration in full cells.

Li3N powder shows good compatibility with Li metal and halide electrolyte. However, commercial Li3N has poor conductivity (~10^{-5} S/cm) without high temperature densification due to the low-conductivity of the α-phase. A planetary ball mill was used to convert the α-Li3N to β-Li3N and reduce particle size. The particle size was reduced from several microns to less than 500 nm. Ionic conductivity increased from 4.3×10^{-5} S/cm for pristine commercial powder to 6.5×10^{-5} for the ball milled powder. Although the ionic conductivity is improved by ca. 50%, it is still lower than the highest conductivity reported in the literature. Ball milled Li3N was tape cast with 3% MSB1-13 binder with a thickness of ca. 10 µm after drying and lamination. This tape was incorporated into a symmetric cell and cycled, Figure 5a. The overpotential is quite high due to the low conductivity of the Li3N, and the cell shorts at very low current density (similar shorting was observed for multiple cells).

A full cell with NMC cathode tape, halide electrolyte, Li3N tape and Li metal was assembled and cycled at a pressure <10 MPa. Unfortunately, the cell shorted while cycling at 0.05C, although the OCV was normal prior to cycling. Li3N is a harder material than halide material and it is challenging to densify the tape at room temperature. Therefore, Li may penetrate the Li3N tape and form a dendrite in the halide layer.

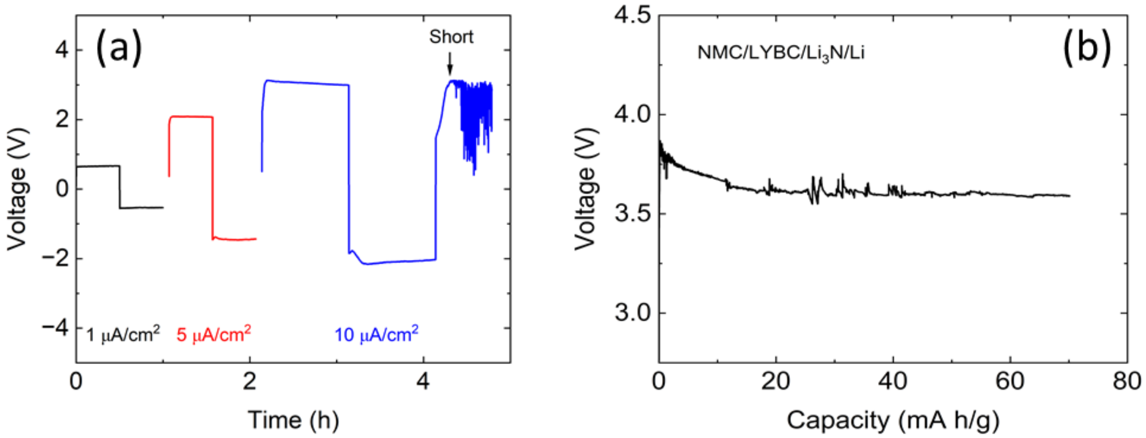

Figure 5. Cells with Li3N interlayers at room temperature. (a) Symmetric Li/Li3N tape/halide tape/Li3N tape/Li cell cycled at 20 MPa and (b) full Li/Li3N tape/halide tape/cathode tape cells cycled at <10 MPa and room temperature.

LPSCl was also considered as an anode interlayer for halide-based cells due to its stable SEI with Li metal. LPSCl tape with 5% PIB binder was obtained from Oak Ridge National Laboratory. All-solid state cells, including NMC cathode tape, halide electrolyte, LPSCl tape and Li metal were assembled and cycled at a very small pressure to avoid Li creep. Charge/discharge curves of one cell are shown in Figure 6. The initial discharge capacity was ca. 56 mAh/g. The cell did not display short circuiting in the first 20 cycles. While this capacity is low, the integration of halide/argyrodite bilayer electrolyte with Li metal is promising, and will be pursued further.

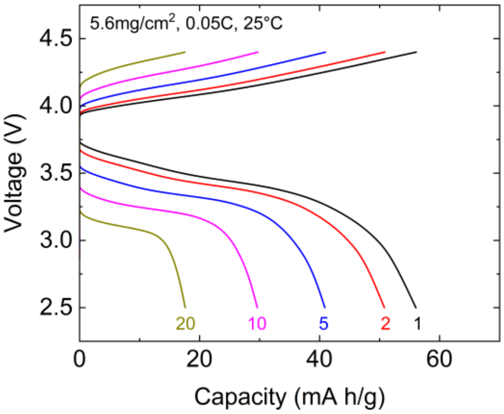

Figure 6. Cycling with LPSCl interlayer. Li (40 µm)/LPSCl (30 µm)/halide (40 µm)/NMC (50 µm). All layers were tape cast, except for the Li metal.

Tape casting

In the previous year, toluene solvent and MSB1-13 binder were selected for tape casting based on their compatibility with halide powder. Milled Gen2.2 powder with a small amount (2 or 3%) of binder was tape cast and the tapes could be peeled off from the substrate after drying, resulting in free-standing tapes >60 cm2. The thickness of the pristine tape is ~57 µm and it decreases to 50 µm after densification via lamination. The free-standing tape with 2% binder was wrapped on stainless steel rods with different diameters, and survived curvature down to 2 mm diameter, shown in Figure 7. The tape also survived folding and unfolding. Upon compression after folding, however, the tape cracked. This means that compressing folded multi-layers in a wound pouch cell to improve capacity becomes challenging and may require more development. It is still possible to stack multi-layers in bipolar-stack pouch cells.

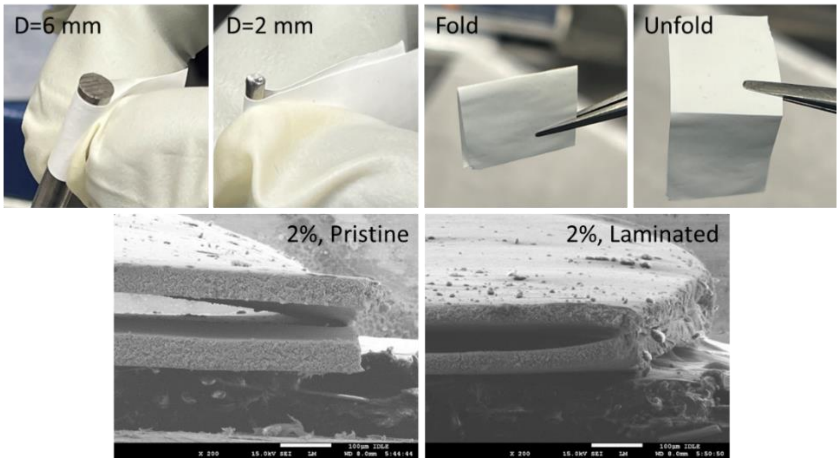

Figure 7. (top) Winding and compression test for a free-standing halide tape. (bottom) SEM images after folding and pressing on the folded edge.

Using the cathode materials selected above, a cell was fabricated with all tape-cast layers, Figure 8. The cathode was tape cast with 80% NMC811, 18% nano LIC catholyte, 1% C65 and 1% MSB1-13 binder. Gen2.2 electrolyte was tape cast with 2.5% MSB1-13 binder. A cell with Li-In alloy anode was assembled and tested in a Sphere Energy 0.5 cm^2 cell hardware at 100 MPa. The cell was then cycled at 0.1 C and shows a good retention over 28 cycles. The discharge capacity of the tape cell is lower than the pellet cells showed in Figure 2, which could be ascribed to the higher interfacial resistance caused by the binder in the tapes, and uneven pressure as the hardware is not optimized for such thin cells.

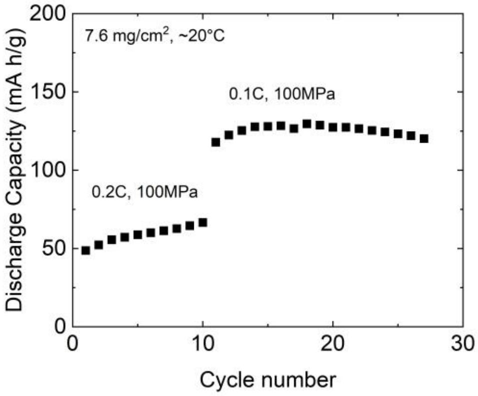

Figure 8. Tape cast cell. Li-In(80µm)/Gen2.2 tape (60µm)/NMC-milled Gen2.2 tape (55µm) cell structure. Rate capacity tests at 0.2 and 0.1 C for the cell with 18% LIC catholyte.

Cell scale-up

A scaled-up cell with optimized electrolyte and cathode was assembled and tested, Figure 9. The cell was 3x4 cm, with LiIn anode, halide tape electrolyte, and halide/NMC/C tape cathode. It was cycled at 20 MPa, 0.1 C (114 µA/cm2) and room temperature. The 1st cycle discharge capacity is 6.0 mA h. After 25 cycles, the testing temperature was then increased to 50 °C and the cell was further cycled at 0.2 C. The discharge capacity increased to 6.9 mA h. The discharge capacity fading at 50 °C is faster than at room temperature, which is consistent with our previous study on halide-based pellet cells. Another pouch cell with the same composition and structure was assembled and cycled at 0.05 C, the 1st discharge capacity increases to 7.1 mA h. The remainder of the project will focus on improving pouch cell performance.

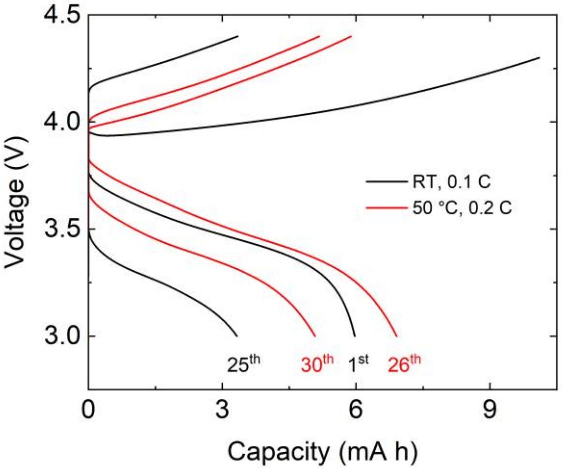

Figure 9. The cycle charge/discharge curves of a 3x4 cm cell. Cycles 1-25 at room temperature and 0.1C; cycles 26-30 at 50°C and 0.2C. (Specific discharge capacity at the 1st cycle: 87.2; 25th cycle: 48.6; 26th cycle: 100.8; and 30th cycle: 74.2 mA h/g).